Astron. Astrophys. 73, 1–13 (1979)

ASTRONOMY AND ASTROPHYSICS

Line Profiles in Expanding Envelopes

J. Surdej

European Southern Observatory, Casilla 16317, Santiago-9, Chile

Received May 29, revised July 19, 1978

Summary. Using Sobolev-type approximations for the transfer of line radiation in expanding envelopes, a great variety of computed line profiles are presented and described in the frame of a two-level atom model. The calculated fluxes are those emerging from outward-accelerating (or equivalently inward-decelerating) and outward-decelerating (or equivalently inward-accelerating) envelopes under different general assumptions (spherical velocity distributions of the type $V(r)=V_0(1/L)^l$, constancy of the ionization balance across the envelope, etc.) when the only source of excitation is that due to the pure resonance scattering of line photons.

We briefly discuss the possible interpretation of observed line profiles in terms of geometrical and physical parameters prevailing in the envelopes. Namely, it is shown that for some cases the type of velocity field, the dimensions of the atmosphere, the radial optical depth τ_{12}^l and occasionally the mass-loss rate may be deduced from the analysis of one line profile.

Key words: moving stellar envelopes – radiative transfer – line profiles – emission-line stars – quasars

1. Introduction

While it is generally accepted to interpret P-Cygni line profiles as formed by extended envelopes expanding around a stellar core, very little is yet known about the driving mechanisms responsible for the outflow of matter as well as for the possible effects of an underlying chromosphere (cf. Magnan, 1977). One of the basic problems we investigate in the present paper is how to infer, under simplified hypotheses, the physical and geometrical parameters prevailing in expanding media from the analysis of one or several individual observed line profiles.

Recently many authors have proceeded to calculations of line profiles emerging from outward-accelerating envelopes, hereafter referred to by A.E (Castor, 1970; Lucy, 1971; Kuan and Kuhi, 1975; Oegerle and van Blerkom, 1976; etc.), from outward-decelerating envelopes, henceforth referred to by D.E (Kuan and Kuhi, 1975; Grachev and Grinin, 1975; Marti and Noerdlinger, 1977; Rybicki and Hummer, 1978; etc.) and, equivalently, from inward-accelerating envelopes (Bertout, 1977; etc.) using Sobolev-type approximations for the transfer of the line photons. Though intensive calculations of line profiles illustrate most of these works, no thorough attempt has been made for interpreting the most dependent features of a line profile in relation with the physical structure of the radiating gas.

We propose here such an analysis for spherical velocity distributions of *power law* type. The general hypotheses assumed throughout this work are laid down in Chapt. 2. A first approach, aiming to apply a general method in order to infer atmospheric parameters directly from observations of P-Cygni lines (resonance transition), is presented in Chapt. 3.

The difficulties encountered by taking into account the *occultation* and *inclination* effects and the spatial transfer of line photons in D.E. envelopes led us to expose more general equations for computing line profiles in Chapt. 4. For uniformity, we show how these equations can be derived through results obtained in previous works (Surdej, 1977; Surdej, 1978a; Surdej, 1978b, respectively referred to below as Papers I, II, III) though they have been established earlier by Castor (1970), for the case of A. E. envelopes, and by Kuan and Kuhi (1975), for D. E. envelopes, in a different formalism. In Chapt. 4 too, computed line profiles in A.E. and D.E. envelopes are displayed for various sets of physical and geometrical parameters specific to the media and, finally, a complete discussion of the results and conclusions form Chapt. 5.

2. General Hypotheses

Let us recall briefly the general hypotheses assumed here when dealing with the formation of line profiles in the context of the *Sobolev approximation* (Sobolev, 1947, 1957, 1958). A more detailed discussion of these may be found in the previous articles (Papers I, II and III).

In the following, either we consider spherical envelopes around a stellar core which are in rapid expansion or contraction with either a positive or negative radial velocity gradient. The level-populations of the flowing atoms have reached a steady state and, in the frame of a moving atom, the emitted photons are completely redistributed in frequency and direction. $\Phi(\nu-\nu_{12})$ represents an arbitrary function describing the interaction of the two levels (1 denoting the lower and 2 the upper one) with line photons around the central frequency ν_{12} of the transition. In order to clearly set forth the specific roles due to spectral line formation, geometrical effects, etc. in the moving gas, only radiative exchanges in the transition $1\rightarrow 2$ are taken into account. To avoid further complexities (choice of temperature distribution, transfer of ionizing radiation, etc.) no attempt has been made for treating the ionization balance of the atomic species under consideration.

In the present work we adopt velocity distributions of the type

$$V(r)=V_0(1/L)^l \qquad (1)$$

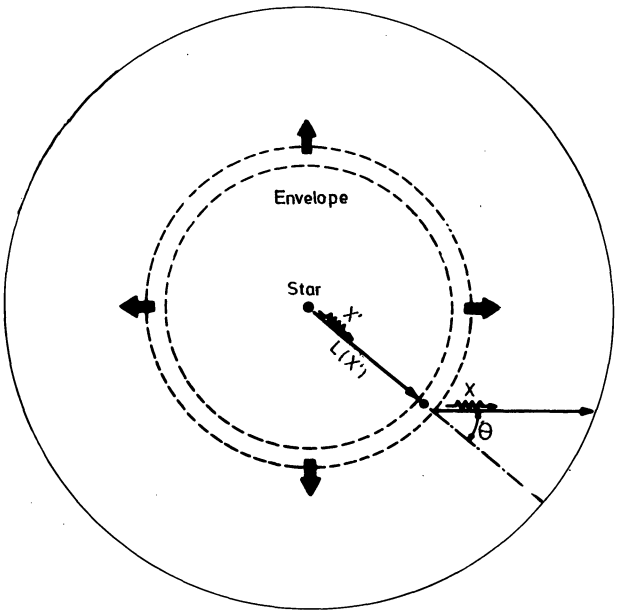

Fig. 1. Geometry in an expanding envelope around a punctual star (see text). No scale is respected

where

$$L=r/R^* \tag{2}$$

expresses the radial distance r to the central star in stellar radii R^* units. V_0, a positive constant (respectively negative), represents the radial velocity at the stellar surface for flows directed outwardly (respectively inwardly) and l is an accelerating parameter (respectively decelerating) when negative (respectively positive).

Finally, the shape of the underlying photospheric lines being unknown, we considered for simplicity that the stellar core radiates continuously, like a black body at temperature T, without limb darkening and with an intensity I_c constant over the line frequency.

3. Formation of Line Profiles: First Approach

In this chapter we shall present a simple but rigorous approach to the problem of line formation in A.E. envelopes. The reasoning we adopt consists in following the fate of a stellar photon as it crosses the A.E medium before reaching an observer. Analytic expressions for the line profile function will be derived all along the discussion and will enable to understand the most dependent features of a line profile. Finally, we shall show the complexity arising in D.E. envelopes when one attempts to follow a similar reasoning.

The only source of excitation being due to the pure resonance scattering of the stellar photons, a new energy distribution in frequency of the stellar continuum will result as a consequence of the large Doppler shifts of the absorbing and emitting atoms across the medium. The new observed spectrum of stellar radiation will lie within the frequency interval $\nu\in[\nu_{\min}, \nu_{\max}]$ given by the Doppler relation

$$\frac{\nu-\nu_{12}}{\nu_{12}}=\frac{V(r)}{c}\cdot\cos\theta, \tag{3}$$

where the extreme frequencies $\nu_{\min}$ and $\nu_{\max}$ of the emitted line photons are those respectively due to atoms receding and approaching the observer along the line of sight with the maximum velocities $-V_{\max}$ and $V_{\max}$. In relation (3) the constant c stands for the light velocity and θ measures the angle between the radial direction and that of light propagation.

Let X be the dimensionless frequency defined by

$$X=\frac{-(\nu-\nu_{12})}{(\nu_{\max}-\nu_{12})}, \tag{4}$$

such as the frequency interval is now $X\in[-1, 1]$.
Combining (3) and (4) we derive the useful relation

$$X=-\frac{V(r)}{V_{\max}}\cdot\cos\theta. \tag{5}$$

A. Isotropy and Punctual Star

In the first step we shall concentrate on the following model: an envelope, extending up to an upper limit $L=L_{\max}$, is outward-accelerated with the same rate ($l=-1$) in all directions around a punctual stellar core. Because of the presence of a radial velocity gradient we easily understand that a stellar photon emitted at a frequency X' (all frequencies being defined with respect to a frame at rest, if not stated otherwise!) will have a certain probability $P(X')$ to be absorbed locally in the atmosphere at a certain distance $L(X')$ as long as $X'\in[-1, X_{\min}]$, $X_{\min}$ referring to the greatest frequency at which stellar photons may interact with the outwardly ejected atoms. For $\theta=0$, relation (5) gives

$$L(X')=(-X')^{-\frac{1}{l}}\cdot L_{\max}, \tag{6}$$

from which we deduce

$$X_{\min}=-L_{\max}^{l}. \tag{7}$$

The fraction $P(X')$ of first absorbed stellar photons will then diffuse locally any number n ($n=0, 1, 2, \ldots$) of times with a probability $(1-\beta_{12}^1)^n$ (see Paper II) but will finally leave locally the whole envelope isotropically and, as a consequence, equally distributed over the frequency interval $[X', -X']$. Indeed, the intrinsic emission of line radiation by atoms is isotropic in our model and we further assumed that the medium is physically the same in all directions ($l=-1$). Therefore the escaping photons, being emitted over all directions $\theta\in[0,\pi]$ with the same probability, will appear in the frame of an observer with their frequencies X equally redistributed in the range $X\in[X', -X']$ (see relation (5) and Fig. 1). We can now deduce that all scattered line photons reaching an observer with a frequency X can only be due to those stellar photons initially radiated with a frequency X' such as

$$X'\leqq-|X|.$$

From our discussion it finally results that the fraction $E_1(X)/E_c$ of absorbed stellar photons and $E_2(X)/E_c$ of non-absorbed stellar photons, initially emitted by the punctual core in constant numbers over frequencies $X'\in[-1,1]$ and reaching an observer with a frequency X are respectively given by

$$\frac{E_1(X)}{E_c}=\int_{\mathrm{Max}(|X|,\,-X_{\min})}^{1}\frac{P(X')}{2X'}\,dX', \tag{8}$$

$$\frac{E_2(X)}{E_c}=1-P(X) \quad \text{if} \quad X\in[-1, X_{\min}]$$

and

$$\frac{E_2(X)}{E_c}=1 \quad \text{if} \quad X\in[X_{\min}, 1]. \tag{9}$$

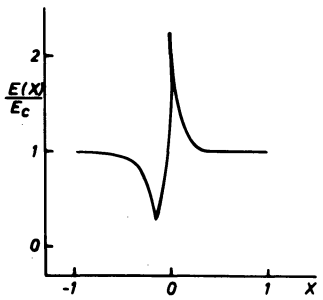

Fig. 2. Line profile as a function of frequency X for the case of an A.E envelope around a punctual star with parameters $l=-1$, $\tau_{12}^{l}=10^3$ and $L_{\max}=50$

From the theory exposed in Paper I it is easy to calculate the probability $1-P(X')$ that a stellar photon of frequency $X'\in[-1, X_{\min}]$ will cross radially the whole moving envelope without being absorbed locally somewhere. We shall anticipate the demonstration of this result [see relations (29) and (31)] which leads to

$$1-P(X')=\exp(-|\tau_{12}|), \tag{10}$$

where $|\tau_{12}|$ is the fictive optical depth evaluated at the point $(L=L(X'), \theta=0)$ of possible interaction.

The total fraction $E(X)/E_c$

$$\frac{E(X)}{E_c}=\frac{E_1(X)+E_2(X)}{E_c} \tag{11}$$

of scattered and non-scattered stellar photons contributing to a frequency X is merely the line profile function normalised to the stellar continuum. Combining relations (6)–(10) and relations (42), (43) and (44) from Paper II for the particular case $l=-1$, it comes that

$$\left.\begin{array}{l}\text{if}\quad X\in\left[-1,\dfrac{-1}{L_{\max}}\right],\\ \\ \text{if}\quad X\in\left[-\dfrac{1}{L_{\max}},1\right],\end{array}\right\}\quad \frac{E(X)}{E_c}=\int_{\operatorname{Max}\left(|X|,\frac{1}{L_{\max}}\right)}^{1}\frac{\left(1-\exp\left(-\dfrac{\tau_{12}^{l}}{L_{\max}^{3}X'^{3}}\right)\right)}{2X'}\cdot dX'+\left\{\begin{array}{l}\exp\left(\dfrac{\tau_{12}^{l}}{L_{\max}^{3}X^{3}}\right)\\ \\ \\ 1\end{array}\right., \tag{12}$$

where τ_{12}^{l} is the radial optical depth at the stellar surface.

Equation (12) was solved for the values of the parameters $L_{\max}=50$ and $\tau_{12}^{l}=10^3$. The corresponding line profile in Fig. 2 was calculated within $10^{\min}$ with an HP-25 pocket calculator. The line profile displayed in Fig. 2, mainly composed by a central emission located at $X=0$ and a shortward displaced absorption at $X=X_{\text{abs}}$, has been often observed in the emission-line spectra of various peculiar objects (P-N, novae, W-R and Be stars, QSO's, etc.), the most representative of which is P-Cygni, a former nova of the XVII century.

We may naturally wonder about the possible analysis of a given P-Cygni line profile (resonance line) in terms of the physical and geometrical parameters τ_{12}^{l}, V_0, $L_{\max}$, etc. We shall see hereafter that if the medium is expanding isotropically ($l=-1$) around a point-like star, Eq. (12) gives an unambiguous determination of the latter parameters. Let us remark immediately that, contrary to some past claims, the position X_{abs} of the extremum in the P-Cygni absorption does not correspond necessarily to the velocity of ejection V_0. Indeed, in Fig. 2 we have $X_{\text{abs}}=0.14$ rather than $X_{\min}=0.02$.

Our short analysis will first consist in evaluating the derivative of the function $E(X)/E_c$ [relation (12)] and, noticing that the former is null for $X=X_{\text{abs}}$, we shall seek for relations between the parameters X_{abs}, τ_{12}^{l} and $L_{\max}$. For $X\in[-1, X_{\min}]$ we find

$$\frac{d}{dX}\left(\frac{E(X)}{E_c}\right)=\frac{\left(\exp\left(\dfrac{\tau_{12}^{l}}{L_{\max}^{3}X^{3}}\right)-1\right)}{2X}-3\cdot\exp\left(\frac{\tau_{12}^{l}}{L_{\max}^{3}X^{3}}\right)\cdot\frac{\tau_{12}^{l}}{L_{\max}^{3}X^{4}}. \tag{13}$$

When nullifying the derivative, we have equivalently

$$\exp(-Y)\cdot(1+6Y)-1=0 \tag{14}$$

with $Y=|\tau_{12}^{l}/(L_{\max}^{3}X^{3})|$.

Using the Newton-Raphson method, we solved Eq. (14) and obtained the non-trivial root $Y^*=2.918300476$. Consequently,

$$X_{\text{abs}}=-\left(\frac{\tau_{12}^{l}}{L_{\max}^{3}\cdot Y^*}\right)^{1/3}. \tag{15}$$

With the last relation and by trials we may guess the value of $\tau_{12}^{l}/L_{\max}^{3}$ which makes possible a good fit between the residual intensity $E(X)/E_c$ [see relation (12)] evaluated at $X=X_{\text{abs}}$ and the residual intensity observed on the analysed profile. Similarly, using expression (12) it is possible to find the value of $L_{\max}$ which fits the maximum intensity $E(X)/E_c$ for $X=0$ with the observed one.

Finally, the knowledge of $\tau_{12}^{l}/L_{\max}^{3}$, X_{abs}, $1/L_{\max}$ and the velocity V_{abs} of the absorption component measured in the P-Cygni profile suffices to calculate the values of the parameters $L_{\max}$, τ_{12}^{l}, $V_{\max}$ and V_0.

Let us point our attention on the condition $X_{\text{abs}}\in[-1, X_{\min}]$ explicitly assumed when establishing relation (15). Using definitions (7) and (15), the latter condition implies

$$Y^*<\tau_{12}^{l}<Y^*L_{\max}^{3}. \tag{16}$$

This last condition means namely that if the medium is optically thin $|\tau_{12}(L=1)|<Y^*$ at the stellar surface, we have $X_{\text{abs}}=X_{\min}$ and only in this case $V_{\text{abs}}=V_0$. On the other hand, if the medium is optically thick at the edge of the envelope $|\tau_{12}(L_{\max})|>Y^*$, we have $X_{\text{abs}}=-1$ and $V_{\text{abs}}=V_{\max}$.

Though we illustrated the last case in some of the next figures, it is very unlikely to encounter a physical envelope with a steep cut-off at $L=L_{\max}$ where $|\tau_{12}(L_{\max})|>Y^*$.

B. Generalisation

We aim to generalise formula (12) to the cases of A.E envelopes for any value of the parameter l. When $l\neq\pm1$, the medium looses its geometrical and physical properties of isotropy. A stellar

photon radiated at a frequency $X' \in [-1, X_{\min}]$, absorbed locally at a distance $L(X')$ with a probability $P(X')$, will be re-emitted with a frequency $X \in [X', -X']$ in a direction θ after any number n ($n=0, 1, 2, \ldots$) of local diffusions with a probability $P(X', X)/|2X'|$ where

$$P(X', X) = \frac{(1-\exp(-|\tau_{12}|))}{|\tau_{12}|} + \frac{(1-\exp(-|\tau_{12}|))(1-\beta^1_{12})}{|\tau_{12}|} + \frac{(1-\exp(-|\tau_{12}|))(1-\beta^1_{12})^2}{|\tau_{12}|} + \ldots,$$

or

$$P(X', X) = \frac{(1-\exp(-|\tau_{12}|))}{\beta^1_{12}}. \quad (17)$$

In relation (17), the fictive optical depth $|\tau_{12}|$ is evaluated at a distance $L = L(X')$ along the direction θ while the escape probability β^1_{12} depends only on $L(X')$. From Eq. (5) we deduce the relation existing between the frequency X and the angle θ

$$X = X' \cdot \cos\theta. \quad (18)$$

A similar demonstration to the one which led to Eq. (12) gives the following expression $E(X)/E_c$ for the general case $l < 0$,

$$\left.\begin{array}{l}\text{if } X \in [-1, X_{\min}],\\ \text{if } X \in [X_{\min}, 1],\end{array}\right\} \quad \frac{E(X)}{E_c} = \int_{\mathrm{Max}(|X|, -X_{\min})}^{1} \frac{P(X') \cdot P(X', X)\, dX'}{2X'} + \begin{cases}\exp(-|\tau_{12}(L(X), \theta=0)|)\\ 1\end{cases}. \quad (19)$$

Let us notice for the particular case $l = -1$ that $P(X', X) = 1$.

In parallel to our investigation exposed in Chap. 3.A concerning the fitting of an observed line profile with a synthetic one, we shall just outline that a similar analysis still remains possible for the general case $l < 0$.

Using the previous results and those obtained in Chap. 3.A of Paper II, we can calculate the asymptotic expressions for $E(X)/E_c$ when $|\tau_{12}| \gg 1$ and $|\tau_{12}| \ll 1$ throughout the envelope. Adopting the same conditions for the ranges of frequencies as those in Eqs. (12) and (19), we find

i) if $|\tau_{12}| \gg 1$,

$$\frac{E(X)}{E_c} \simeq \int_{\mathrm{Max}(|X|, -X_{\min})}^{1} \frac{1}{2X'\beta^1_{12}|\tau_{12}(L(X'), \theta(X))|}\, dX' + \begin{cases}0\\ 1\end{cases}$$

or

$$\frac{E(X)}{E_c} \simeq \frac{3}{(2-l)} \int_{\mathrm{Max}(|X|, -X_{\min})}^{1} \left|\frac{1-(l+1)\left(\frac{X}{X'}\right)^2}{2X'}\right| dX' + \begin{cases}0\\ 1\end{cases}$$

and, finally,

$$\frac{E(X)}{E_c} \simeq \frac{3}{(2-l)}\left[\frac{(l+1)X^2(1-\mathrm{Max}(|X|, -X_{\min})^{-2})}{4} - \frac{1}{2}\ln(\mathrm{Max}(|X|, -X_{\min}))\right] + \begin{cases}0\\ 1\end{cases} \quad (20)$$

ii) if $|\tau_{12}| \ll 1$,

$$\frac{E(X)}{E_c} \simeq \int_{\mathrm{Max}(|X|, -X_{\min})}^{1} \frac{|\tau_{12}(L(X'), \theta=0)|}{2X'}\, dX' + \begin{cases}1-|\tau_{12}(L(X), \theta=0)|\\ 1\end{cases}$$

or

$$\frac{E(X)}{E_c} \simeq \frac{\tau^l_{12} L^{2l-1}_{\max}}{2} \int_{\mathrm{Max}(|X|, -X_{\min})}^{1} X' \frac{1-3l}{l}\, dX' + \begin{cases}1-\tau^l_{12} L^{2l-1}_{\max}|X|^{\frac{1-2l}{l}}\\ 1\end{cases}$$

and, finally,

$$\frac{E(X)}{E_c} \simeq \frac{\tau^l_{12} L^{2l-1}_{\max}}{2}\left(\frac{l}{1-2l}\right)\left(1-\mathrm{Max}(|X|, -X_{\min})^{\frac{1-2l}{l}}\right) + \begin{cases}1-\tau^l_{12} L^{2l-1}_{\max}|X|^{\frac{1-2l}{l}}\\ 1\end{cases}. \quad (21)$$

Applications of formulae (20) and (21) respectively for the sets of parameters $l = -0.5$, $L_{\max} = 50$, $|\tau_{12}| \gg 1$ and $l = -0.5$, $L_{\max} = 50$, $\tau^l_{12} = 0.1$ are illustrated in Figs. 3 and 4.

C. The Core Effects

In order to complete the first approach of line formation in A.E envelopes we must admit that the approximation of a punctual stellar core is no longer valid when investigating the radiative processes close to the stellar surface.

Indeed, at a certain distance L from the core a certain fraction of emitted line photons, roughly proportional to the dilution factor W, will be back-scattered towards the star and will thus remain unobservable. In the frame of an observer, these lost photons will have positive frequencies $X \in [0, 1]$ and a gap in the red wing of the observed line profile will result. This is the *occultation effect*.

Another effect due to the finite size of the core is that atoms situated at a distance L will interact with the stellar photons not only along the radial direction, but also along directions such as $\theta \in [0, \arcsin(1/L)]$. We shall call this the *inclination effect*.

Formula (19) could be easily modified on account of both these effects.

D. Outward-decelerating Envelopes

As we outlined in the previous works, a spatial transfer of line photons will occur between distant parts of a D.E envelope. A

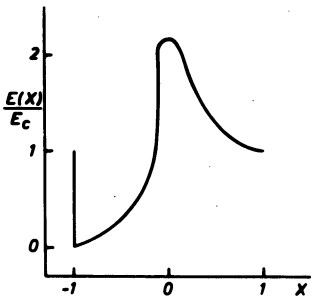

Fig. 3. Line profile as a function of frequency X for the case of an A.E envelope around a punctual star with parameters $l=-0.5$, $|\tau_{12}| \gg 1$ and $L_{max}=50$

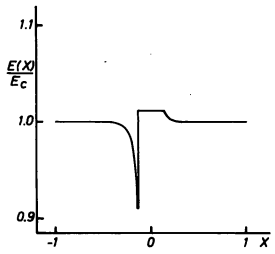

Fig. 4. Line profile as a function of frequency X for the case of an A.E envelope around a punctual star with parameters $l=-0.5$, $\tau_{12}^{l}=0.1$ and $L_{max}=50$

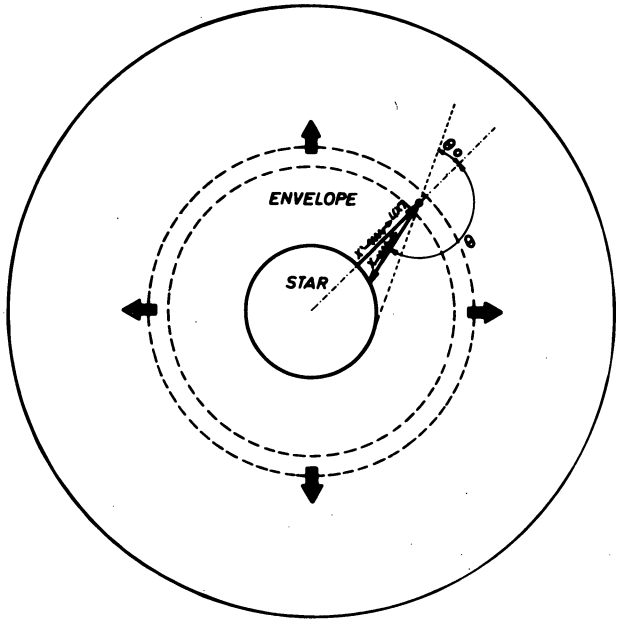

Fig. 5. Geometry in an expanding envelope around a stellar core (see text). No scale is respected

stellar photon radiated at a frequency X' and absorbed around a point P_0 with a probability $P(X')$ may not only diffuse locally but also towards distant points P_0', whose relative velocity to P_0 is null. Because of these random motions of the line photons between different physical parts of a D.E envelope it is no longer possible to define a simple analytic function for the line profile $E(X)/E_c$ as we did in the case of A.E envelopes. Furthermore, because the radial velocity gradient decreases outwardly in D.E envelopes, the interactive processes taking place close to the star will influence the line profile within an appreciable range of frequencies. Therefore, the occultation and inclination effects will play a major role in D.E envelopes. The more general approach of line profile formation exposed in the next chapter will allow to overcome easily these difficulties.

4. General Equations

We have seen in the preceding chapter that a first approach which consisted in following the fate of a stellar photon as it crosses the atmosphere enabled to derive simple expressions for the line profile function in A.E envelopes. We shall present here a more general method applicable to both A.E and D.E envelopes and which automatically includes the occultation and inclination effects.

Two steps may be distinguished in this method. In the first one we solve the statistical equilibrium equation in order to evaluate the source function s_{12} and the fictive optical depth $|\tau_{12}|$ across the atmosphere. This problem was fully exposed and solved in Papers I and II. The physical conditions being known over the whole space of the envelope, we now calculate for each frequency $X \in [-1, 1]$ the total amount of energy $E(X)$, defined per frequency and solid angle units, radiated by the medium towards a fixed observer. The quantity $E(X)$ is then simply given by the integration of the monochromatic intensity function $I(X)$, implicitly space-defined, over a plane perpendicular to the line of sight

$$E(X)=\iint I(X)\,d\Sigma. \tag{22}$$

In the frame of a fixed observer $I(X)$ accounts for the intensity of line radiation emitted along a direction parallel to the line of sight by those parts of the envelope presenting a constant Doppler shift [see relation (5)]

$$V(r)\cos\theta=-X\cdot V_{max}.$$

This last equation was solved for different values of $X \in [-1, 1]$ and the resulting *surfaces of equal frequency* as seen by a fixed observer are illustrated in Figs. 6–8 for the cases of A.E envelopes with $L_{max}=20$; $l=-0.5$, -1, -2 and in Fig. 9–11 for the cases of D.E envelopes with $L_{max}=5$; $l=0.5$, 1, 2.

Because of the symmetry existing around the line of sight, Eq. (22) simplifies to

$$E(X)=2\pi\int_0^{r_{max}} I(X)\,P\,dP, \tag{23}$$

where $I(X)$ is evaluated over the surface of equal frequency X and where the cylindrical coordinate P is defined by

$$P=r\cdot\sin\theta. \tag{24}$$

Normalising $E(X)$ to the integrated stellar flux E_c

$$E_c=2\pi\int_0^{R^*} I_c\,P\,dP, \tag{25}$$

the line profile function $E(X)/E_c$ is merely expressed by

$$\frac{E(X)}{E_c}=2\int_0^{L_{max}}\frac{I(X)\,L\,p\,dLp}{I_c}, \tag{26}$$

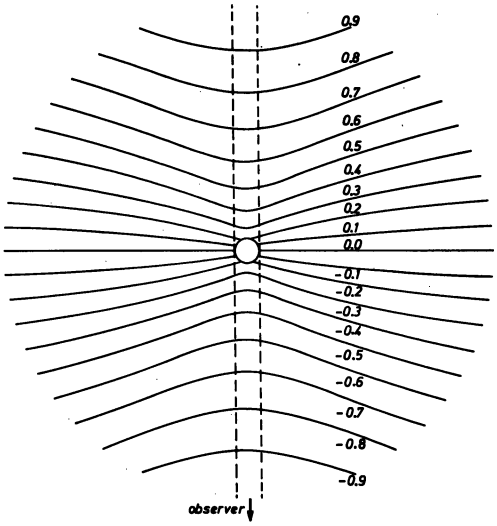

Fig. 6. Surfaces of equal frequency X in an A.E envelope with parameters $l=-0.5$, $L_{max}=20$

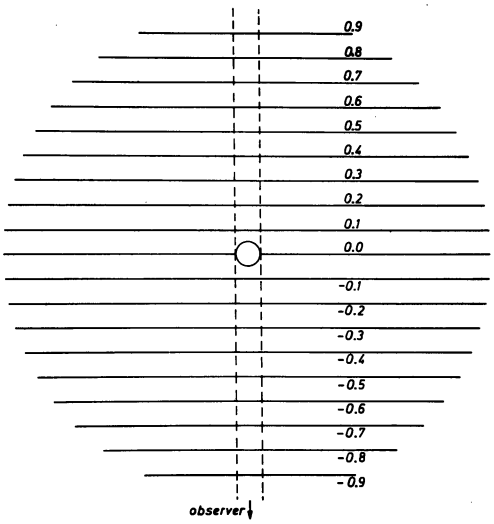

Fig. 7. Surfaces of equal frequency X in an A. E envelope with parameters $l=-1$, $L_{max}=20$

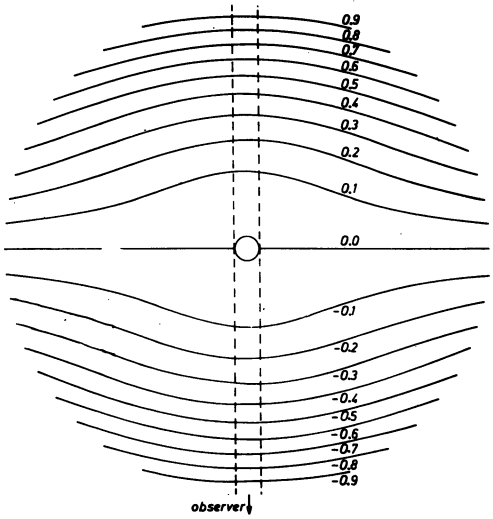

Fig. 8. Surfaces of equal frequency X in an A.E envelope with parameters $l=-2$, $L_{max}=20$

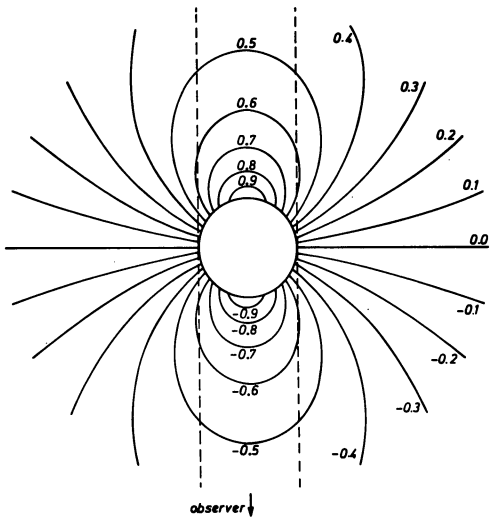

Fig. 9. Surfaces of equal frequency X in a D.E envelope with parameters $l=0.5$, $L_{max}=5$

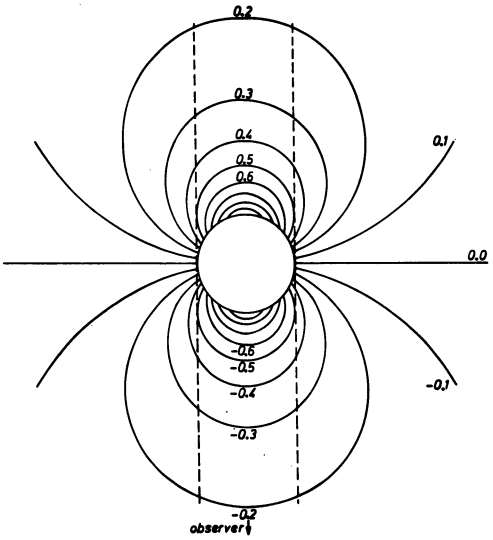

Fig. 10. Surfaces of equal frequency X in a D.E envelope with parameters $l=1$, $L_{max}=5$

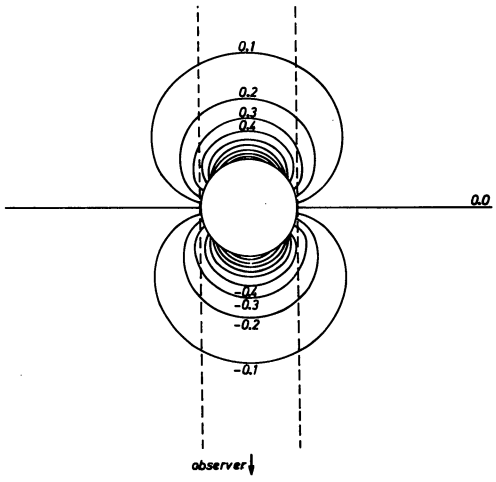

Fig. 11. Surfaces of equal frequency X in a D.E envelope with parameters $l=2$, $L_{max}=5$

where

$$Lp=\frac{P}{R^*}. \tag{27}$$

For convenience, we may separate distinct parts of the gas which bring contributions to the line profile in A.E and D.E envelopes. Because of the outward expansion, the gas confined between the star and the observer (see the region between the dashed lines in Figs. 6–11) partly emits line photons at negative frequencies towards the observer and partly absorbs the emerging stellar radiation. In the following we shall denote $E_1(X)/E_c$ and $E_3(X)/E_c$ respectively those contributions to the line profile function. The gas located in the two lobes exterior to the dashed lines will radiate photons at both negative and positive frequencies due to the approaching and receding motions of the atoms. The quantity $E_2(X)/E_c$ will refer to this specific part of the line profile function.

A. A.E *Envelopes*

Following similar considerations to those developed in Chaps. 3 and 4 of Paper I concerning the derivation of the specific intensity of line radiation emitted at a frequency X and escaping the neighbourhood of a point in the envelope [see formula (2.4)], we can directly write the expression of the function $I(X)$ appearing in formula (26).

As far as the emission of line photons by the gas along a direction of abscissa s is concerned we find

$$I(X)=\int_{s_1(X)}^{s_2(X)} \varepsilon_{12}\Phi\left(-\frac{v_{12}}{c}\cdot\frac{\partial Vs}{\partial s}\cdot s\right) \cdot\exp\left(-\int_{s}^{s_2(X)}\alpha_{12}\Phi\left(-\frac{v_{12}}{c}\cdot\frac{\partial Vs}{\partial s}\cdot s'\right)ds'\right)ds, \tag{28}$$

where $s_1(X)$, $s_2(X)$ are the abscissae enclosing the neighbourhood from which atoms can emit line radiation entering Eq. (28). This so-called neighbourhood lies around the point of intersection between the line of sight for a given Lp and the surface of equal frequency X. In Eq. (28), ε_{12} and α_{12} denote the volume emission and absorption coefficients and $\partial Vs/\partial s$ the velocity gradient along the given direction.

If $Lp\leqq 1$, we must add the contribution due to the stellar continuum absorbed in the neighbourhood $[s_1(X), s_2(X)]$

$$I(X)=I_c\cdot\exp\left(-\int_{s_1(X)}^{s_2(X)}\alpha_{12}\Phi\left(-\frac{v_{12}}{c}\cdot\frac{\partial Vs}{\partial s}\cdot s\right)ds\right), \tag{29}$$

the exponential factor representing the probability that a stellar photon emitted at frequency X will cross unhindered the neighbourhood $[s_1(X), s_2(X)]$.

The integrations in Eqs. (28) and (29) may be performed directly by using simple transformations (see transformations (7.4) and (8.4) in Paper I). We shall not detail these calculations but refer the reader to Paper I.

The final results are, for Eq. (28),

$$I(X)=S_{12}(1-\exp(-|\tau_{12}|)) \tag{30}$$

and for Eq. (29),

$$I(X)=I_c\exp(-|\tau_{12}|). \tag{31}$$

Combining these results with Eq. (26), the line profile function reduces to

$$\frac{E(X)}{E_c}=\frac{E_1(X)+E_2(X)+E_3(X)}{E_c} \tag{32}$$

or, if $X\in[-1, 0[$

$$\frac{E(X)}{E_c}=2\left[\int_0^{L_{\max}}\frac{S_{12}}{I_c}\cdot(1-\exp(-|\tau_{12}|))LpdLp +\int_0^1\exp(-|\tau_{12}|)LpdLp\right] \tag{33}$$

and if $X\in[0, 1]$

$$\frac{E(X)}{E_c}=2\left[\int_1^{L_{\max}}\frac{S_{12}}{I_c}\cdot(1-\exp(-|\tau_{12}|))LpdLp+\frac{1}{2}\right].$$

Let us notice that for $X\in]0, 1]$, the occultation effect and the full transparency of the envelope in front of the star have been taken into account.

B. D.E *Envelopes*

Figures 6–8 and 9–11 show the net difference between surfaces of equal frequency in A.E and D.E envelopes. Indeed, although there is always a unique point of intersection between a direction parallel to the line of sight and a surface of equal frequency in the case of A.E envelopes, two such intersections may occur in D.E envelopes. Having in mind this possible interaction between two distant parts of the atmosphere, we must correct accordingly relation (33) when expressing the line profile function in D.E envelopes. We obtain, if $X\in[-1, 0[$,

$$\frac{E(X)}{E_c}=2\left[\int_0^{L_{\max}}\left(\frac{S_{12}}{I_c}(1-\exp(-|\tau_{12}|))\exp(-|\tau'_{12}|) +\frac{S'_{12}}{I_c}(1-\exp(-|\tau'_{12}|))\right)LpdLp +\int_0^1\exp(-|\tau_{12}|)\exp(-|\tau'_{12}|)LpdLp\right] \tag{34}$$

and, if $X\in[0, 1]$,

$$\frac{E(X)}{E_c}=2\left[\int_1^{L_{\max}}\left(\frac{S_{12}}{I_c}(1-\exp(-|\tau_{12}|))\exp(-|\tau'_{12}|) +\frac{S'_{12}}{I_c}(1-\exp(-|\tau'_{12}|))\right)LpdLp+\frac{1}{2}\right].$$

If, for a given Lp, the line of sight intersects the surface of equal frequency once, we equate to zero the quantity $|\tau'_{12}|$ in Eq. (34).

C. Results

Eqs. (33) and (34) were solved rigorously for various sets of the parameters l, τ_{12}^l and $L_{\max}$. The results are illustrated in Figs. 12–16 for the cases of A.E envelopes and in Figs. 17–21 for D.E envelopes. Each of these figures contains four graphs. The first graph displays the resulting line profile function $E(X)/E_c$ against the frequency $X\in[-1, 1]$. The three other ones inform about the individual contributions, respectively $E_1(X)/E_c$, $E_2(X)/E_c$ and $E_3(X)/E_c$.

Table 1 summarises the sets of parameters used for the calculations of each line profile. In that table, column 1 gives the figure number, column 2 a label (a, b or c) specific to each line profile. Finally, columns 3, 4 and 5 indicate the values of the parameters l, τ_{12}^l, and $L_{\max}$.

5. Discussion

Under the hypothesis that the stellar core is punctual and because the only source of excitation is due to the scattering of line

Figs. 12–21. See Table 1 for captions

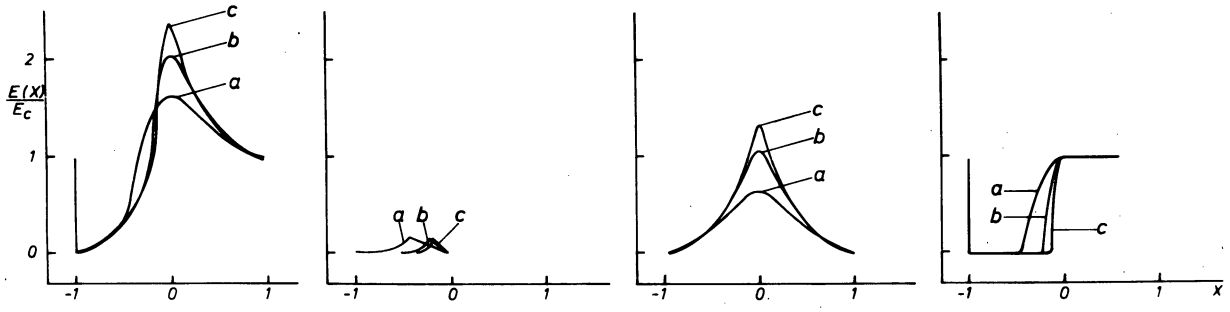

Fig. 12.

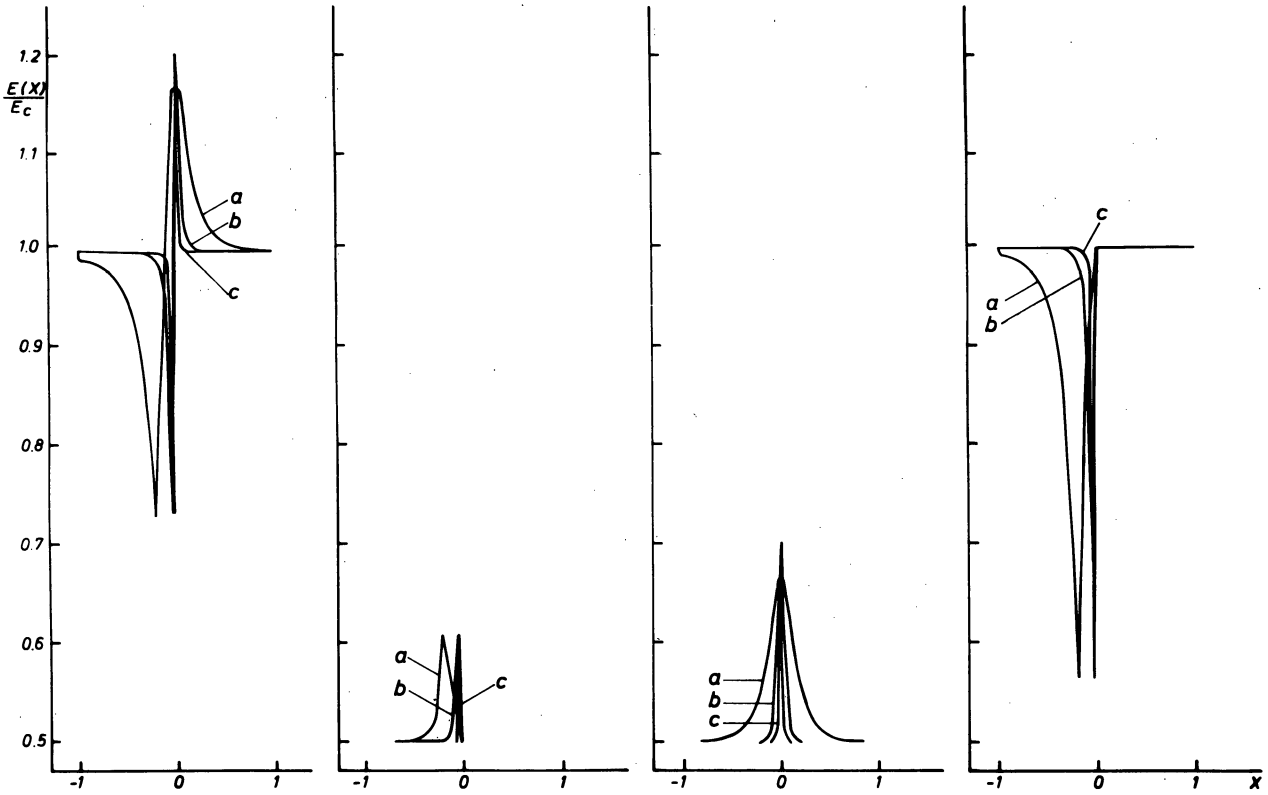

Fig. 13.

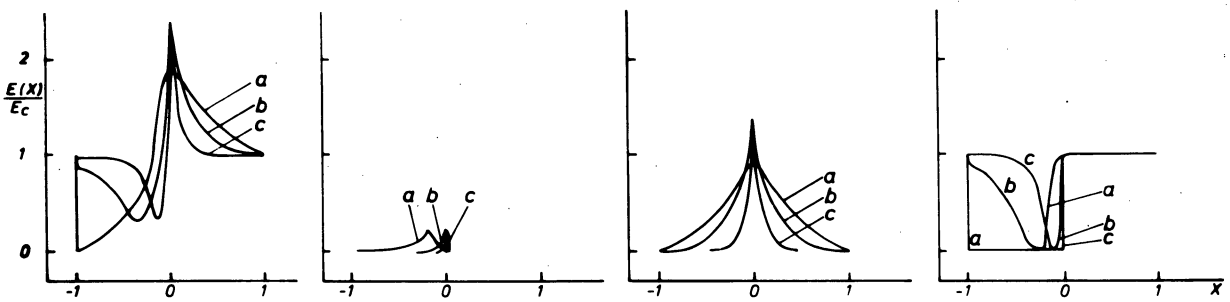

Fig. 14.

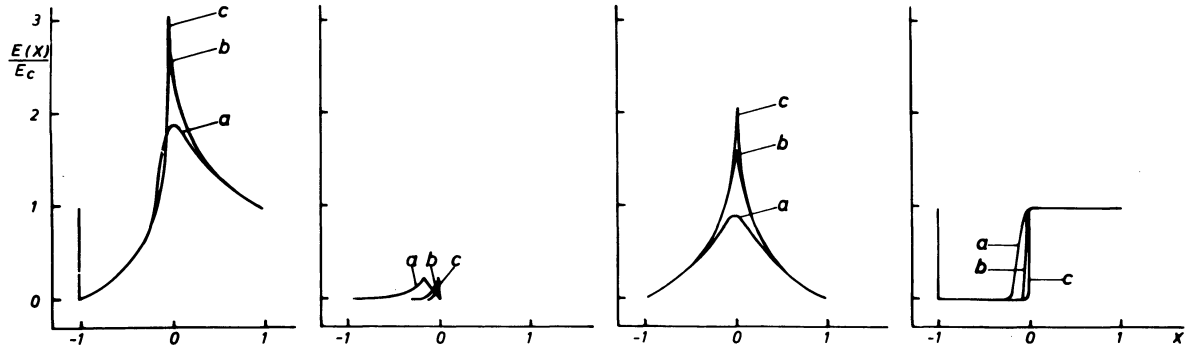

Fig. 15.

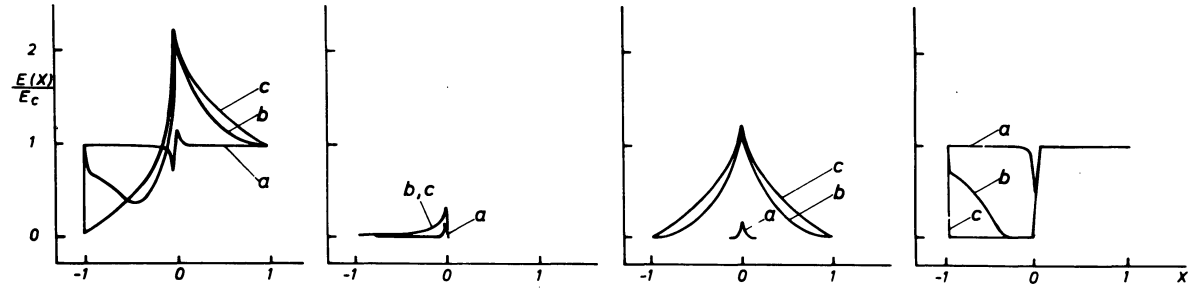

Fig. 16.

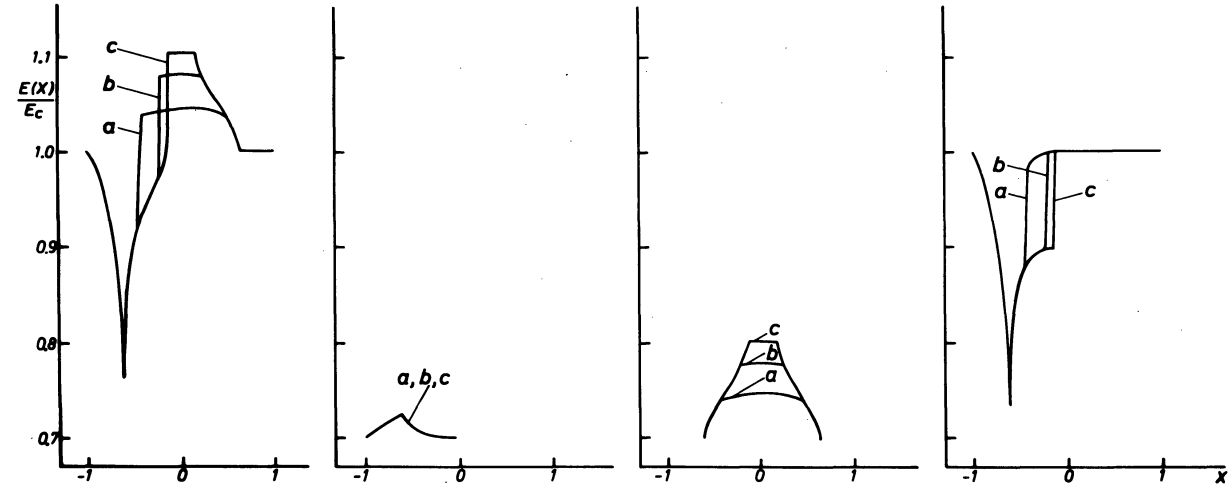

Fig. 17.

photons, the balance of energy in the system *star plus envelope* implies that we must have equality between the equivalent widths of the emission E_{EW} and absorption E_{AB} components of a line profile. This condition is fulfilled for the line profiles in Figs. 2–4 (see Chap. 3).

Because of the occultation by the stellar core of the rear half part of the atmosphere (see Figs. 6–11) we have, for all line profiles displayed in Figs. 12–21

$$E_{EW} < E_{AB},$$

the part played by the occultation effect being quantitatively represented by the area $\int_{-1}^{0} E_1(X)/E_c dX$ in each second graph of Figs. 12–21.

Let us remark that the transformation $X \rightleftarrows -X$ would result in interpreting the surfaces of equal frequency and the corresponding line profiles as formed by collapsing envelopes, inward-decelerated (Figs. 6–8, 12–16) and inward-accelerated (Figs. 9–11, 17–21).

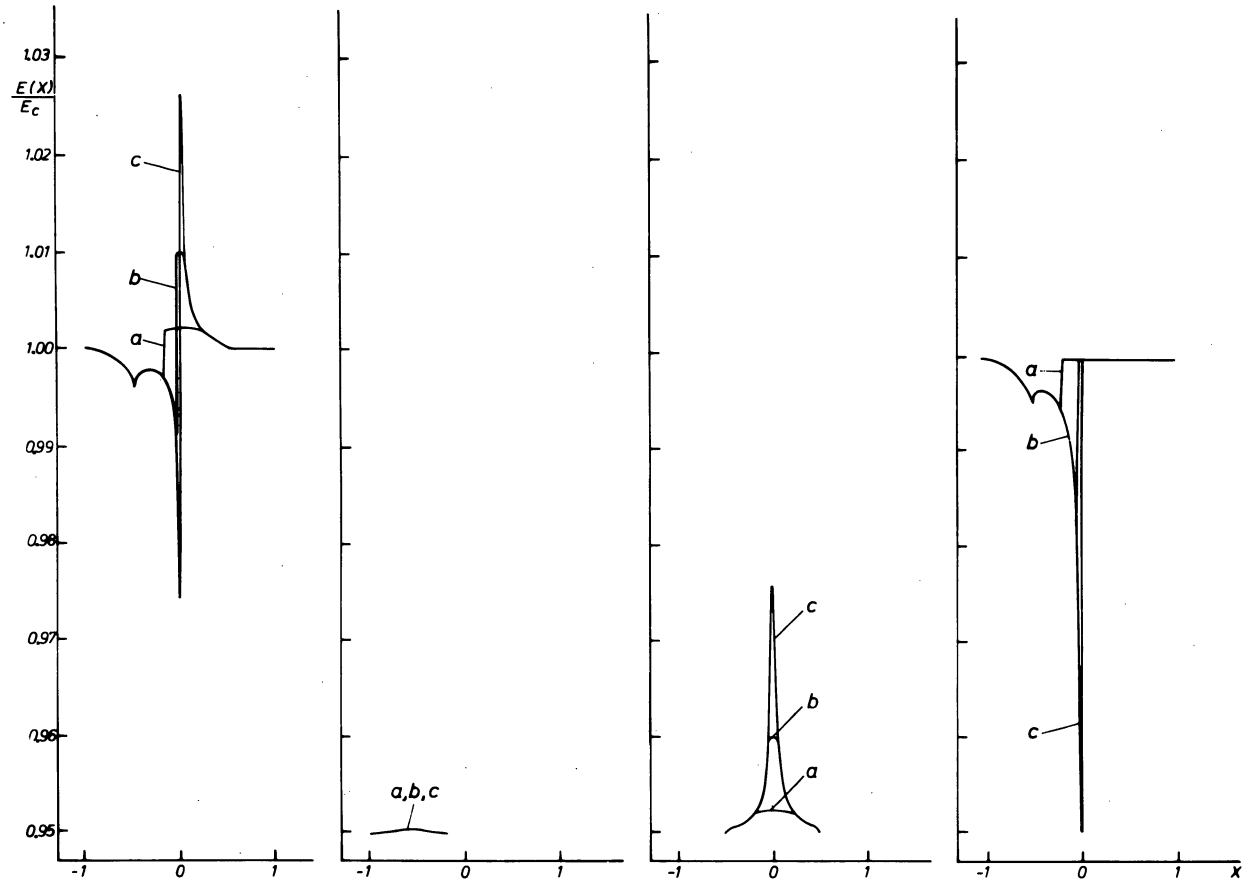

Fig. 18.

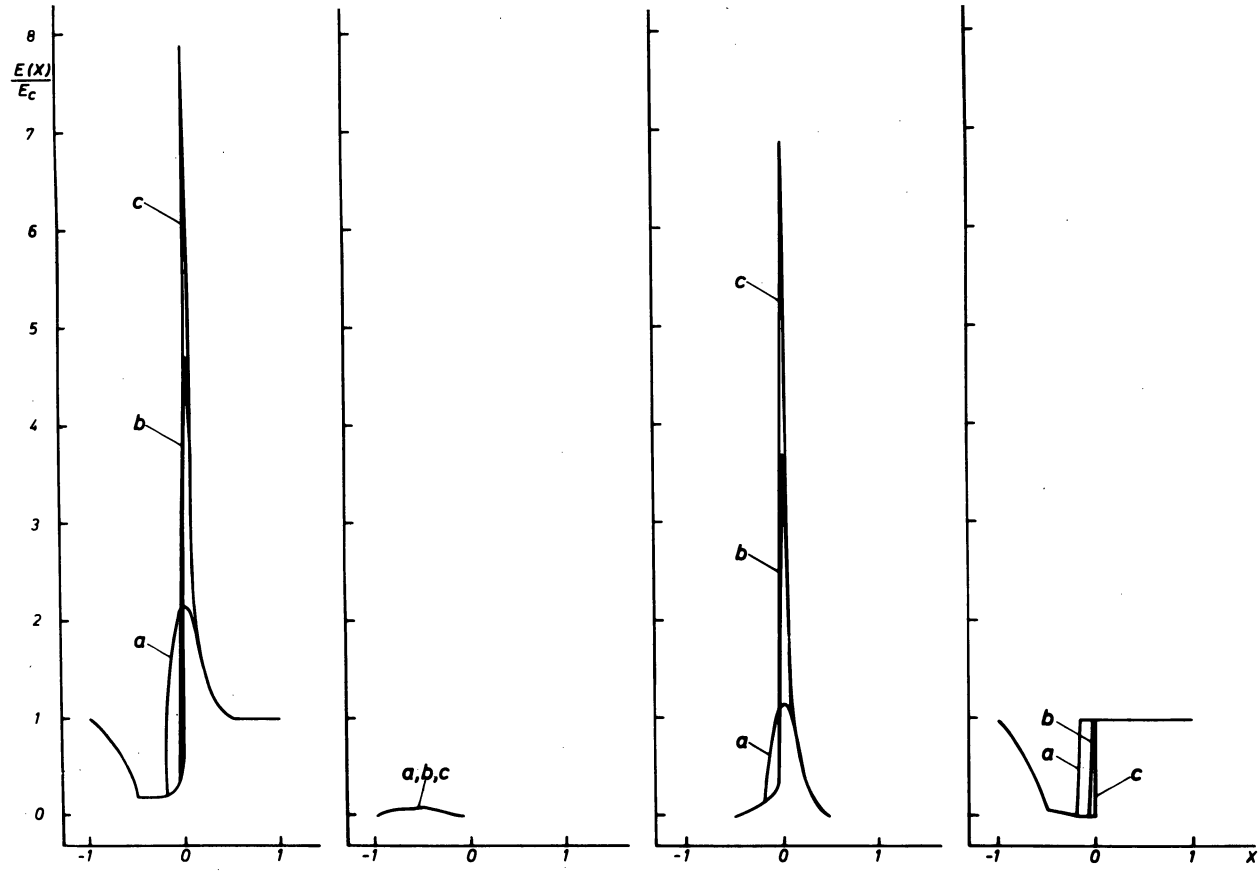

Fig. 19.

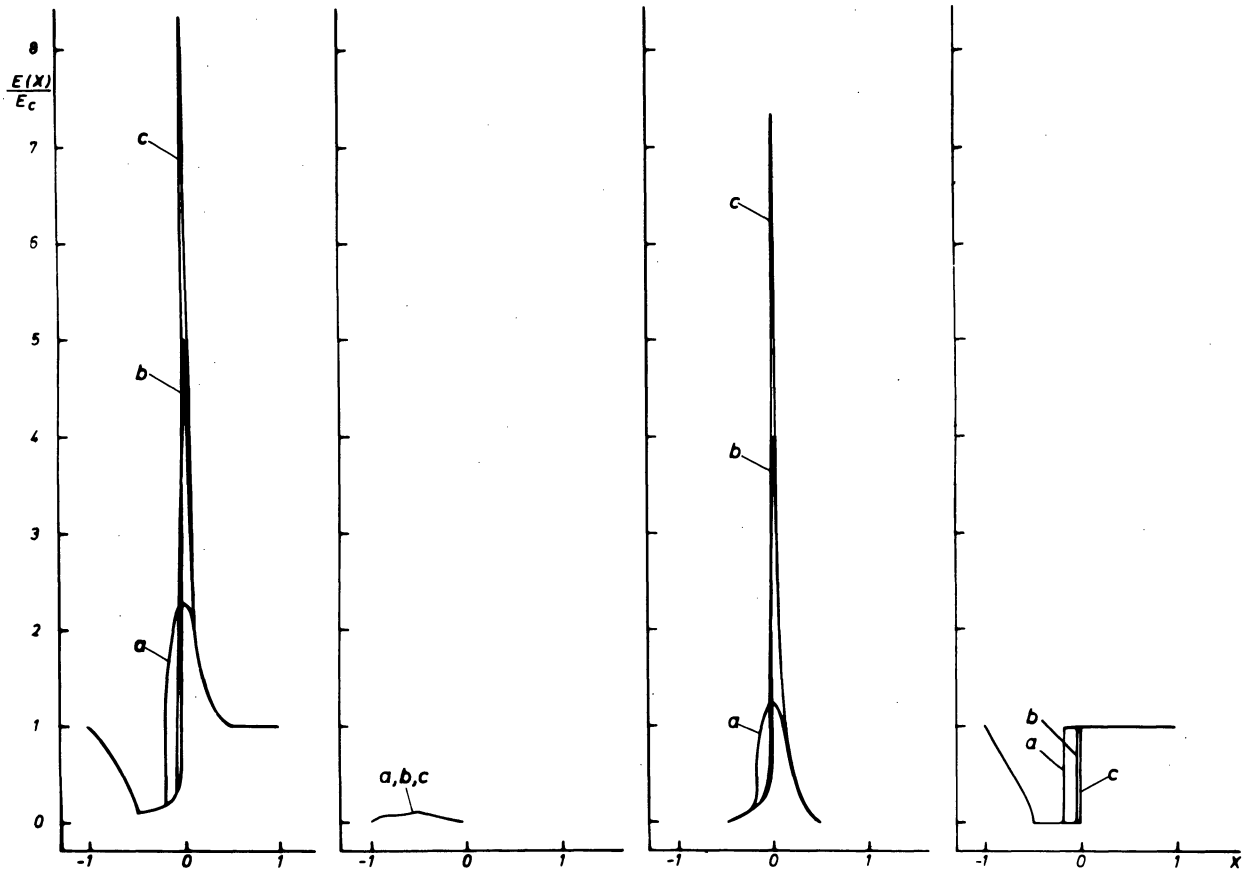

Fig. 20.

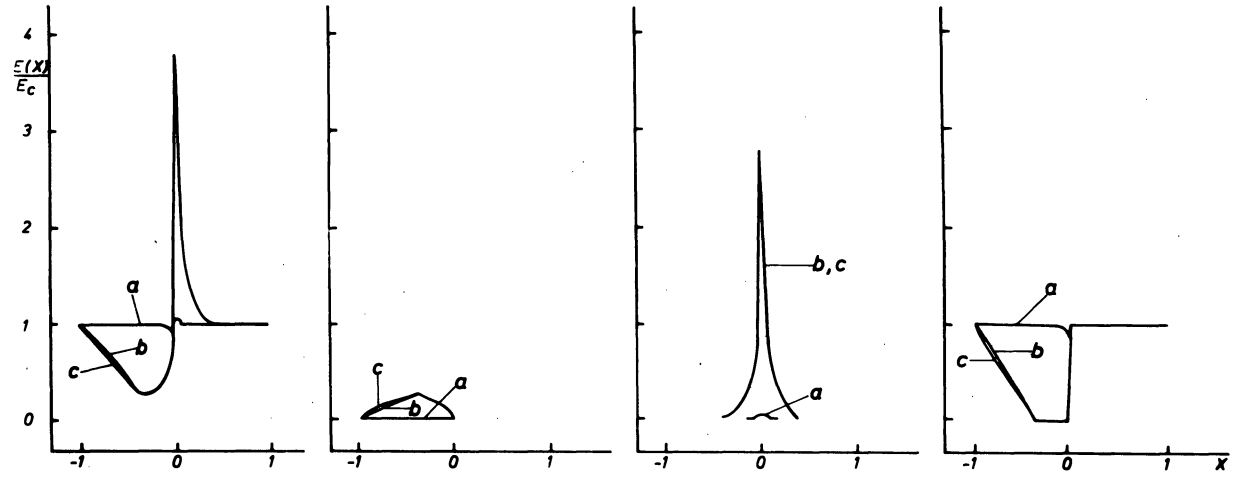

Fig. 21.

A. A.E *Envelopes*

The most important part of the discussion concerning the formation of line profiles in A.E envelopes has been given in Chap. 3.

B. D.E *Envelopes*

The general appearance of line profiles formed in D.E envelopes is striking (see Figs. 17–21): an abrupt transition from the emission peak to the P-Cygni absorption component as well as a sharp cut of the red wing (occultation effect) affect greatly the shape of these profiles.

Inspection of the surfaces of equal frequency in Figs. 9–11 leads to the following results:

i) The shortest extent of the P-Cygni absorption located at $X=-1$ corresponds to the maximum velocity V_0 of the matter ejected at the stellar surface.

Table 1. References for the presentation of Figs. 12–21 (see Chap. 4)

Figure number	Label	l	τ_{12}^l	L_{max}
12	a	−0.5	10^9	5
	b			20
	c			50
13	a	−1	1	5
	b			20
	c			50
14	a	−1	10^3	5
	b			20
	c			50
15	a	−1	10^9	5
	b			20
	c			50
16	a	−2	1	5
	b		10^3	
	c		10^9	
17	a	0.5	10^{-1}	5
	b			20
	c			50
18	a	1	10^{-3}	5
	b			20
	c			50
19	a	1	1	5
	b			20
	c			50
20	a	1	10^3	5
	b			20
	c			50
21	a	2	10^{-3}	5
	b		1	
	c		10^3	

ii) The occultation effect becomes total for the closed surfaces of equal frequency $X \in [X_c, 1]$ where [see relation (5)]

$$X_c = \frac{-\cos\theta_c}{L_c^l}$$

with [see relation (44) from Paper II]

$$\cos\theta_c = -(l+1)^{-1/2}$$

and

$$L_c \sin\theta_c = 1.$$

Combining these three relations we find that

$$X_c = \left(\frac{l}{(l+1)}\right)^{\frac{l}{2}} (l+1)^{-1/2}. \tag{35}$$

This important equation allows the decelerating parameter l to be directly determined. For the respective values $l = 0.5, 1, 2$ we have $X_c = 0.620, 0.500, 0.385$.

iii) for $l \geqq 0.5$, the fictive optical depth $|\tau_{12}|$ increases monotonically with L and, consequently, the abrupt transition between the P-Cygni absorption and the emission will occur at the frequency X_t

$$X_t = -(L_{max})^{-l}. \tag{36}$$

The decelerating parameter l being known through relation (35), the last relation provides the dimension of the envelope. However, if X_t lies very close to the rest frequency $X = 0$, a great uncertainty will affect the value of L_{max}.

iv) If $l = 0.5$, the fictive optical depth $|\tau_{12}|$ remaining almost constant throughout the D.E envelope, the functions $E(X)/E_c$ and $E_3(X)/E_c$ will be minimum at $X = -X_c$ (see Fig. 17) because the corresponding surface of equal frequency has the largest cross-section between the two dashed lines in Fig. 9. Similarly for $l > 0.5$ a first minimum may occur at $X = -X_c$ (cf. Fig. 18) followed by a second one at $X = X_t$.

v) As outlined in Chap. 3.D., the inclination effect plays a major role in D.E envelopes. Indeed, while neglecting the latter we would expect $E_3(-1)/E_c = 0$ for $\tau_{12}^l > 1$, we almost contradictorily find (see Figs. 19–21) $E_3(-1)/E_c = 1$.

vi) Noticing that the frequency X_0 at which the single surfaces of equal frequency transform into double ones is given by

$$X_0 = (l+1)^{-1/2} L_{max}^{-l}, \tag{37}$$

we understand that for $|\tau_{12}| \gg 1$ the line radiation emitted from the rear part of a double surface will be totally absorbed in the front one. The excitation degree being higher in the front region for $X > X_0$ than in the front one for the opposite frequency $-X$ (see Figs. 9–11), the asymmetry of the function $E_2(X)/E_c$ in Figs. 19–21 is simply interpreted. Quite the contrary, the function $E_2(X)/E_c$ appears fairly symmetric in Figs. 17, 18 and 21a where $\tau_{12}^l \ll 1$.

vii) The surfaces of same frequency being not deformed but just prolonged when one increases the size L_{max} of a D.E envelope, two line profiles formed under the same physical conditions for two different values of $L_{max_1} < L_{max_2}$ will differ mainly at frequencies $X \in [X_t(L_{max_1}), -X_t(L_{max_1})]$. Therefore, increasing the size of a D.E envelope will mainly cause an enhancement of the emission peak as well as a steeper transition between the emission and absorption components (cf. Figs. 17–20). Finally, let us notice that for $\tau_{12}^l \gg 1$ the line profiles remain almost unchanged when varying τ_{12}^l (cf. Figs. 19–21).

In conclusion we summarise the important steps to be followed when interpreting an observed line profile in terms of the geometrical and physical parameters specific of a D.E envelope.

First of all the velocity of ejection at the stellar surface V_0 is deduced from the shortest extent of the P-Cygni absorption in the line profile. The sharp cut in the red wing of the emission line located at a velocity $V_c = X_c V_0$ informs directly about the decelerating parameter l. The dimension L_{max} of the envelope expressed in stellar radii units is estimated from the position $V_t = X_t V_0$ of the steep transition between the emission and absorption components.

On the basis of these first determined parameters, we then solve rigorously Eq. (34) for various choices of the parameter τ_{12}^l until we reach the best fitting. Whether a good agreement can be reached between theory and observations establishes the validity of the proposed model. Finally, the knowledge of the stellar radius R^* could offer the possibility to calculate the mass-loss rate $F_M = 4\pi R^{*2} n_0 V_0$, where n_0 is deduced from the definition of τ_{12}^l (see Paper II).

Acknowledgements. I especially wish to thank R. Huidobro for his helpful reading and typing of the manuscript. I would like to thank R. Donarski and V. Tapia very much for the photography and drawings used in this article.

References

Bertout, C.: 1977, *Astron. Astrophys.* **58**, 153
Castor, J. I.: 1970, *Monthly Notices Roy. Astron. Soc.* **149**, 111
Grachev, S. I., Grinin, V. P.: 1975, *Astrophysics* **11**, 20
Kuan, P., Kuhi, L.: 1975, *Astrophys. J.* **199**, 148
Lucy, L. B.: 1971, *Astrophys. J.* **163**, 95
Magnan, C.: 1977, Méthodes d'Analyse des Observations, (preprint)
Marti, F., Noerdlinger, P. D.: 1977, *Astrophys. J.* **215**' 247
Oegerle, W. R., Van Blerkom, D.: 1976, *Astrophys. J.* 208, 453
Rybicki, G. B., Hummer, D. G.: 1978, *Astrophys. J.* **219**, 654
Sobolev, V. V.: 1947, Moving Envelopes of Stars, Leningrad: Leningrad State University (in Russian); English translation S. Gaposchkin, Cambridge: Harvard University Press
Sobolev, V. V.: 1957, *Soviet Astron.* **1**, 678
Sobolev, V. V.: 1958, Theoretical Astrophysics, ed. V. A. Ambartsumyan, Pergamon Press Ltd., London, Chap. 29
Surdej, J.: 1977, *Astron. Astrophys.* **60**, 303 (Paper I)
Surdej, J.: 1978a, *Astron. Astrophys.* **66**, 45 (Paper II)
Surdej, J.: 1978b, *Astron. Astrophys.* **62**, 135 (Paper III)